A Wind System Based on FEA of an Axial Flux Permanent Magnet Generator and Modular Multilevel Inverter

Maryam SHOKRI[1], Vahid BEHJAT[2,*], Naghi ROSTAMI[3]

[1]*Department of Electrical Engineering, Azarbaijan Shahid Madani University, Tabriz, Iran*
[2] *Department of Electrical Engineering, Azarbaijan Shahid Madani University, Tabriz, Iran*
[3] *Faculty of Electrical and Computer Engineering, University of Tabriz, Tabriz, Iran*

Article Info	Abstract
	This research develops a low speed wind system based on an axial flux permanent magnet generator with distributed winding and circular magnet shape and a modular multilevel inverter. Machine is modeled by 3D finite element method to obtain the characteristics of the machine and calculate the maximum value of the flux density, which is necessary to simulate the dynamic model of the wind system. Detailed model of the inverter and a control method for protecting the voltage balance are described. Finally the performance of the wind system is evaluated by simulating whole model of the system.

1. INTRODUCTION

Currently, wind energy systems due to maturity in technologies are one of the most promising renewable energy resources. Several countries have now considered deployments of wind farms as a part of sustainable energy solutions in energy expanse plans. The main challenges of low speed topologies such as wind systems, are development of low-speed high power generators with suitable power electronics interfaces for capturing and delivering the maximum wind power to the grid. Many papers studied these challenges but in the most of them, system is viewed from a single perspective, only power electronics or only generators.

In [1-5], modeling and control strategies of a Permanent Magnet Synchronous Generator (PMSG) for wind system has been studied. Reference [1] has focused on energy management methods and the speed variations are not considered. [2] has designed and analyzed a double stator Axial Flux Permanent Magnet (AFPM) machine with high torque density for direct drive applications. 3D Finite Element Method (FEM) has been used to study and model the machine. A performance comparison of direct drive PMSG with three phase commonly used winding has been presented in [6]. The characteristics of the machine under circuit fault, and the steady temperature rise using finite element analysis have been studied. Reference [7] has propounded the dynamical voltage and current assignment strategies for a wind system based on Doubly Fed Induction Generator (DFIG) and nine switch converter. In this reference the current and voltage capacities of the considered converter have been determined to the rotor side and grid side, dynamically. Design and optimization of a direct coupled ironless AFPM wind generator has been studied in [8]. A multi objective design has been done by partial swarm optimization to decrease the active material cost and increase the annual energy yield. In [9] a genetic algorithm and an analytical evaluation of objective

*Corresponding author, e-mail: behjat@azaruniv.edu

functions have been used to optimize a coreless stator and double rotor AFPM machine. The maximum torque density, minimum weight of PMs and minimum machine price are obtained by optimizing five objective functions.

[10-14] have investigated the wind system in the point of view of power electronics and control. The control of a bidirectional DC/DC converter of a wind system with back-to-back NPC has been presented in [10]. DC/DC converter controls the DC-link voltage and NPC has been used to get the maximum power from generator and inject it to the grid. Reference [11] has used the technical data to model the wind system. Reference [12] applied a predictive control to a 3-level boost converter for a medium voltage wind system. A medium voltage wind turbine system consisting of a three phase open winding synchronous generator and a modular multilevel cascade converter has been presented in [15]. The operating principles and control methods have been studied by simulation. [16] has presented the behavior analyzing of offshore wind system including Modular Multilevel Converter (MMC) HVDC during DC faults. It has indicated the wind turbine front-end converters reduce the peak and averaging value of the fault current.

Most of the researches have studied wind systems in the point of view of only generator, or only power electronics. In this paper, a low speed wind system is studied of both aspects. In the proposed system, an AFPM machine with circular magnet shaped is used as the generator and a modular multilevel converter is used as the inverter to connect the system to the grid. Pole numbers of the AFPM machines can be simply increased because of their disk type structure. Consequently, the torque density is high in these type machines rather than radial flux machines. Due to high-power density, axial flux machines can be used in low speed wind power units with limited spaces. AFPM machine with sector like shaped magnet produces a trapezoidal shaped back EMF waveform. It can be produced a sinusoidal EMF waveform with sine shaped and circular shaped magnets, but sine shaped magnet is a complex shape from the perspective of practical construction. So, a circular shaped magnet is used as the magnet of the considered generator.

Modular multilevel converters can be expanded to every level without increasing any complexity to the control system. These converters provide to assemble converters with high number of levels which can be connected to the high voltage grids with any necessary transformers. By increasing the number of levels, it can be obtained voltages with better quality and this advantage surmounts the need to high frequency filters. This paper is organized as the following: first a 3D finite element model of the generator is built and the voltage and flux density of the machine is obtained by FEA. Then, the results of 3D FEM are placed in the dynamic model of the machine to simulate the wind system. Then, control strategy of the inverter is presented in details. Finally, whole model of the proposed low speed wind turbine-generator is simulated and connected to the grid. The proposed system is investigated to evaluate the performance of the system.

2. 3D FINITE ELEMENT MODEL OF THE GENERATOR

The considered generator in this study is a 5KW AFPM machine with two stators with distributed winding and one interior rotor. A circular shaped magnet is used as the surface mounted rotor magnets. Machine has 12 poles on the both surfaces of the rotor and 36 slots on each stator. Windings are distributed in the stator slots with slots/pole/phase equal to one. Due to the 3D structure of the AFPM machines, 3D FEM is used to model the considered machine. Because of the periodicity, it is enough to model only 1/12 of the machine structure. In other words, it is enough to model only one pole of the rotor and 3 slots of the stator. Also due to the symmetry, it can be modeled only one stator and half of the rotor. The modeled stakes of the rotor and stator are illustrated in Fig.1 and Fig.2.

A rare earth NdFeB magnet with relative permeability equal to 1.05T at 20° C is used as the permanent magnet of the generator. Material of the rotor disk is a construction steel S232JR and material of the stators core is a steel sheet M600-50A. Stators operate in parallel in star connection. Outer diameter of the machine is 250mm and inner diameter is 150mm. A transient magnetic application with a step value equal to 10-4 is applied to solve the finite element model of the machine. 3D model is coupled to an external circuit and the model of the rotor rotation is applied through the mechanical sets. The boundary conditions for the proposed machine are described in Fig.3 and the necessary parameters for solving the machine model are given in table. 1.
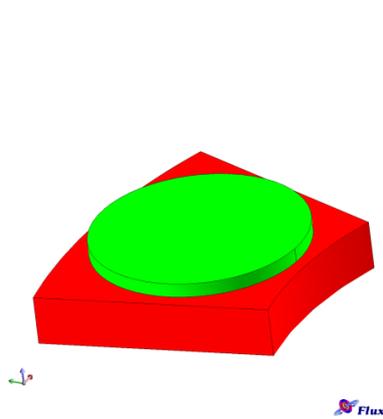
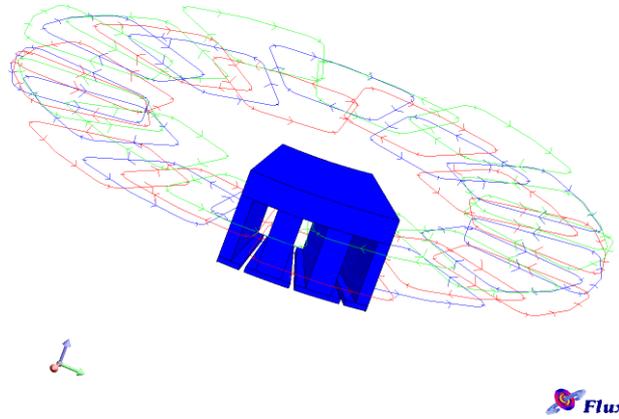*Fig.1.* one pole of rotor of the considered generator

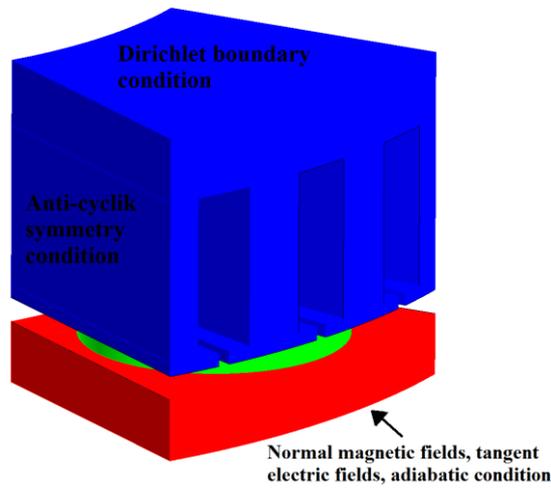*Fig.2.* 1/12 of the one stator and the Distributed winding in the slots

Fig.3 boundary conditions of the studied machine

Table 1. Necessary parameters for solving the model

parameter	Flux 3D by CEDRAT
Number of nodes	47801
Number of line elements	2944
Number of surface elements	58832
Number of volume elements	231576
Mesh order	1st order

Machine voltage and flux density are shown in Fig.4 and Fig.5, respectively. As it can be seen from Fig.4, the voltage of the generator is sinusoidal with good approximation. Also, the voltage harmonics of the proposed machine have been compared with the machines with rectangular and trapezoidal magnet shapes. As it is illustrated in Fig.6, all harmonic components of the machine with circular magnet shape are less than of the other machines harmonics. Magnetic flux distribution at different parts of the rotor and the flux path on the rotor and magnet region are depicted in Fig.7. Maximum flux density in the air gap is 0.852T, nearly. The value of the maximum flux density is required to simulate the dynamic model of the generator in the wind system simulation.
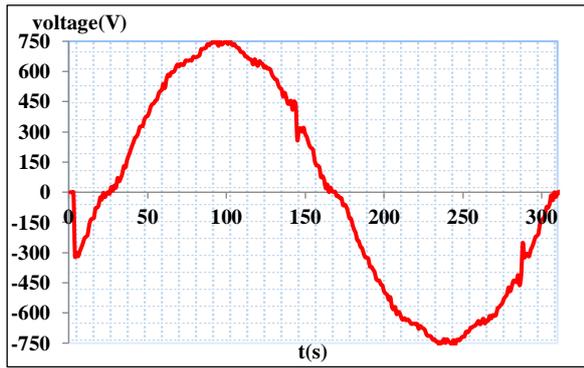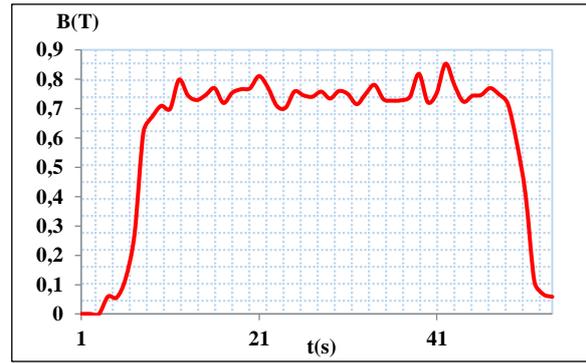
Fig.4. *the phase voltage waveform of the generator*

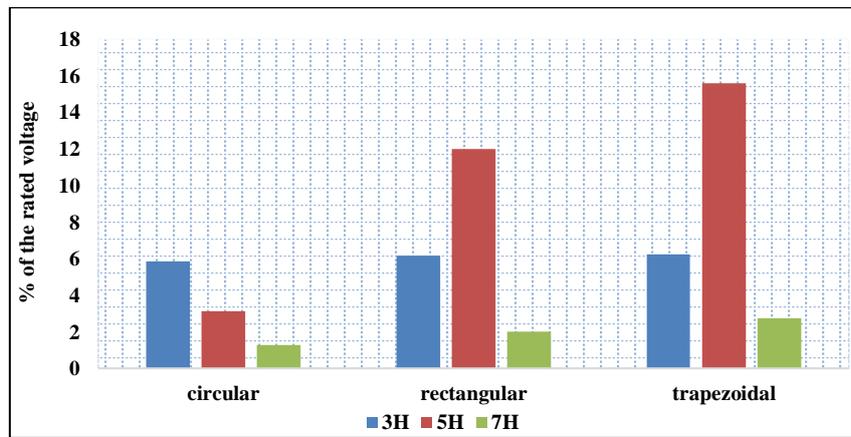**Fig.5.** *the distribution of the flux density of the generator*

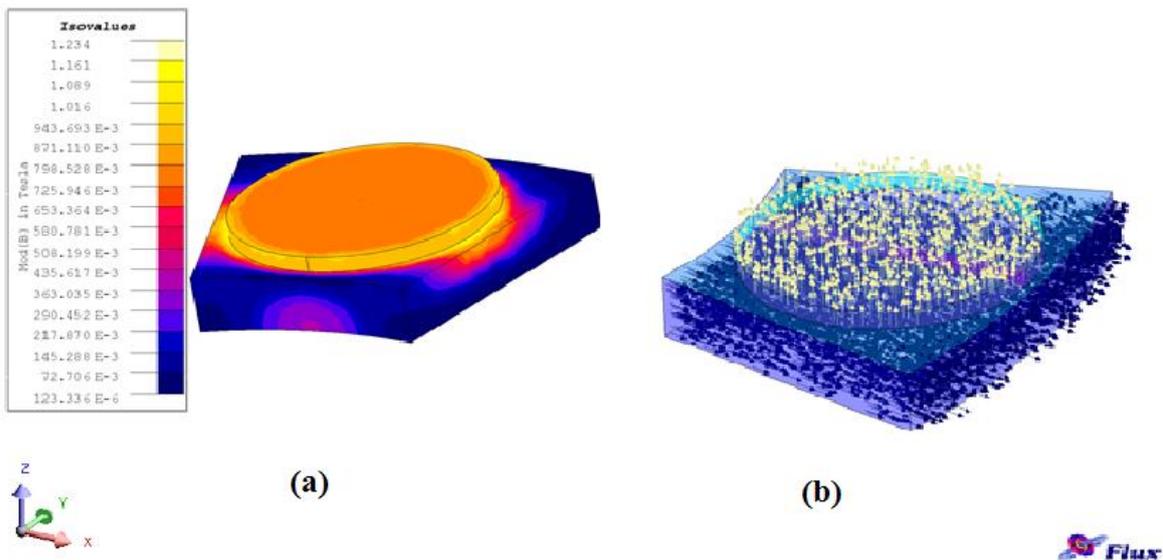**Fig.6.** *compare the harmonics of the machine voltage respect to the magnet shapes.*

Fig.7. *(a) distribution of the magnetic flux density at different part of the rotor. (b) the flux path on the magnet and rotor region after solving the machine model.*

3. THE PROPOSED WIND SYSTEM TOPOLOGY

Fig.8 presents the block diagram of the proposed wind system. The proposed topology is simulated by means of the dynamic model of the components. The dynamic model of the each part is obtained separately, and then whole of the wind system is simulated.
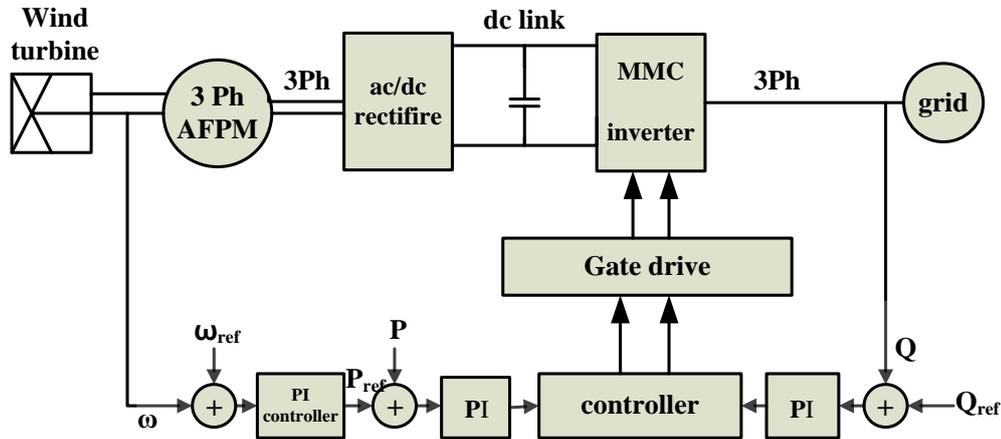

Fig.8 *block diagram of the proposed system*

2.1. Wind-turbine model

In this paper a single mass model of the wind turbine is used to simulate the wind system. a low speed wind turbine is studied in this paper. So that, there is no gearbox between turbine and generator and generally, it is a direct drive wind system. Mechanical power of the wind turbine is:

$$P_m = P_{wind} C_p(\lambda, \theta) \tag{1}$$

$$P_{wind} = \frac{1}{2}\rho A V_w^3 \tag{2}$$

where Pwind is the power of the wind, A is the area swept by the blades, Vw is the wind speed and ρ is air mass density. Cp usually is given by the producers. In this study Cp is considered as a quadratic function, as bellow:

$$C_p = C_{pmax}(1 - (\frac{\lambda}{\lambda_{opt}} - 1)^2) \tag{3}$$

where λ is the tip speed ratio: $\lambda = \frac{R\omega_m}{V_w}$; where R is the turbine diameter and ωm is the mechanical speed.

It can be modeled the turbine-generator connection by the following dynamic equation:

$$T_m - T_e = J\frac{d\omega_m}{dt} + B\omega_m \tag{4}$$

where Tm and Te are the mechanical torque and electromagnetic torque respectively, J is the inertia of the total mass connected to the turbine-generator and B is friction coefficient.

2.2. Dynamic model of the generator

Simulation of the generator is done by using of dynamic equations. The output voltages of the stator in d-q frame are given as follows:

$$V_d = R_1 i_{ad} + L_{sd}\frac{di_{ad}}{dt} - \omega L_{sq} i_{aq} \tag{5}$$

$$V_q = R_1 i_{aq} + L_{sq}\frac{di_{aq}}{dt} + \omega L_{sd}i_{ad} + \omega L_{ad}i_f \tag{6}$$

where Vd, iad and Vq, iaq are voltages and currents of the d and q axes respectively, Lsd and Lsq are synchronous inductances of the d and q axes, R is the stator resistance, ω is the electrical angular speed and if is the equivalent current of the magnet excitation.

Electromagnetic torque of a 3 phases AFPM machine is expressed by the following equation:

$$T_e = \frac{3}{2}p[\varphi_f + (L_{sd} - L_{sq})i_{ad}]i_{aq} \tag{7}$$

where p is the pole pairs and φf is the maximum magnetic flux producing by permanent magnets excitation. This variable is obtained from finite element analysis of the machine that it is calculated equal to 0.852T for proposed generator.

2.3. Model of the inverter

A modular multilevel inverter is used for connecting the wind system to the grid. Generator is connected to the inverter via a 3 phases diode rectifier. Modular multilevel inverters provide to increase the voltage level by increasing the number of modules in each leg, without increasing stresses on the cells. This ability enables these inverters to function in the high voltage systems. The topology of a 4 level modular multilevel inverter is presented in Fig.9. Each cell consists of a chopper cell as it can be seen in the Fig.10. Inverter is switched by the pulse width modulation.
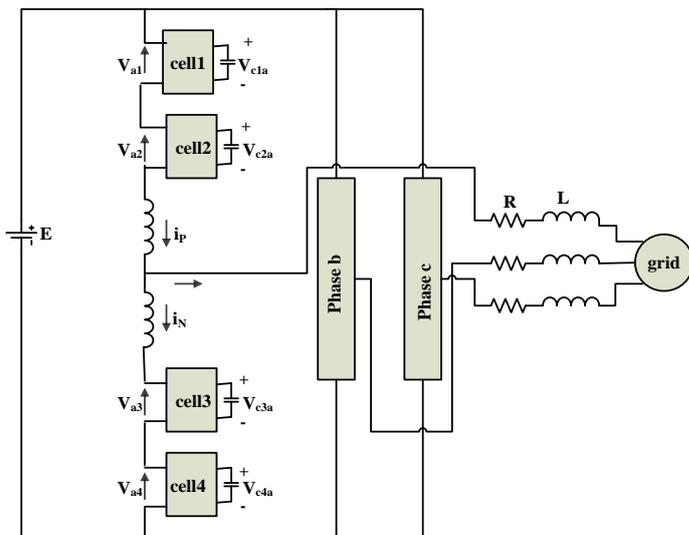

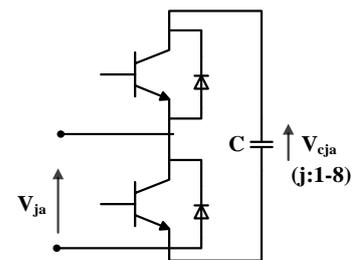**Fig.9.** *configuration of a 4 level modular multilevel inverter*   **Fig.10.** *structure of the each cell*

The most important issue in the modular multilevel inverters is the voltage balance of the chopper cells. To obtain this purpose, an averaging control and a balance control is applied to the inverter. In order to achieve the averaging control, it can be written from the Fig.7:

$$E = \sum_{j=1}^{4} V_{ja} + l\frac{d}{dt}(i_p + i_N) \tag{8}$$

where E is the voltage of the power supply, Vja is the output voltage of each chopper cell, l is the buffer inductance, iP and iN are the positive and negative currents of each leg, respectively. By assuming current iz as follow, it can be controlled the average voltage of the capacitors.

$$i_z = \frac{1}{2}(i_p + i_N) \tag{9}$$

Fig.11 illustrates the block diagram of the average control of the voltage, where VAa* is the obtained command voltage. This block makes the average voltage of the capacitors to track the reference voltage Vc*.
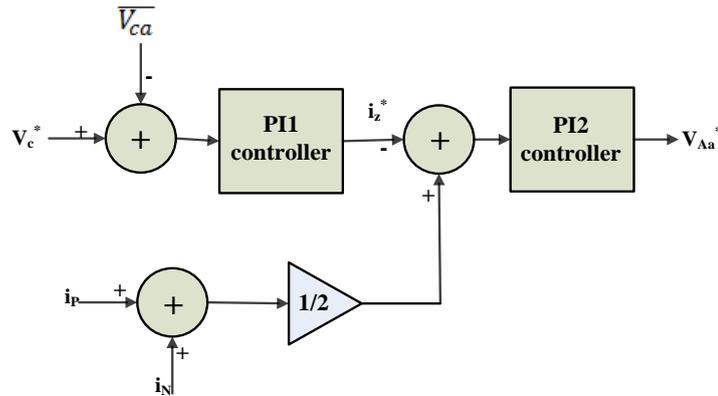

Fig.11. *block diagram of average control*

The average voltage of the capacitors is defined as bellow:

$$\overline{V_{ca}} = \frac{1}{4}\sum_{j=1}^{4} V_{cja} \tag{10}$$

where 'a' points to the phase a. When $V_c^* \geq \overline{V_{ca}}$, then iz* increases and the actual current iz is forced to track the command current iz*. In other words, the feedback control of iz , provides $\overline{V_{ca}}$ to track the Vc* without affecting of the load current. Fig.12 shows the circuit of the balance control. In this circuit, the dc voltage of each cell is forced to track the reference voltage. VBja* is the command voltage that is obtained from the balance control. Balance control is based on iP and iN , so that the polarity of VBja* must be based on polarity variation of iP and iN. Parameters of the inverter are given in table. 2.

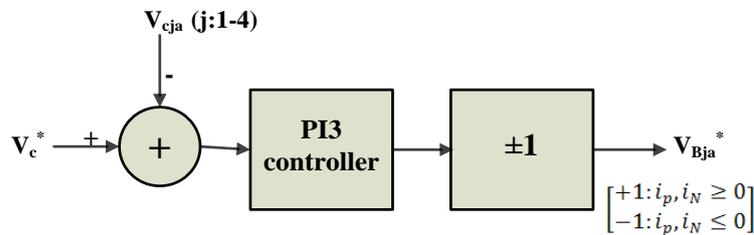**Fig.12.** *block diagram of the balance control*

Table. 2. *Inverter parameters*

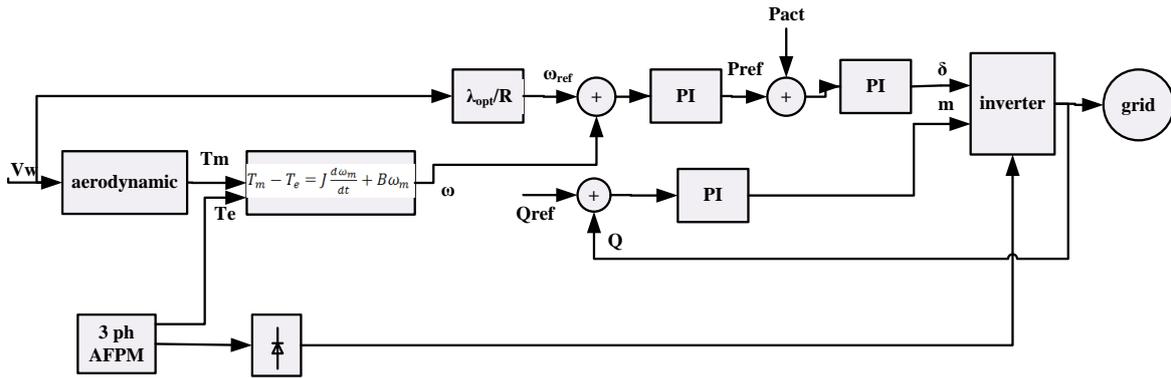|	
Filter inductance	0.1H
Buffer inductance	0.001H
dc capacitor	0.003F
Filter resistance	0.05Ω

Fig.13. *control block diagram of the proposed system*

3. SIMULATION OF THE PROPOSED SYSTEM

Fig.13 depicts the control block diagram of the proposed system. Inverter is switched based on Pulse Wide modulation (PWM). The reference signal of the PWM is built by the following equation:

$$V_t = \frac{\sqrt{2}mV_c}{2}\cos(\omega t + \delta) \qquad (11)$$

m and δ must be determined to obtain this reference signal. The active and reactive power of an inverter with output voltage of Vt and connected to a network with voltage of Vs, are:

$$P = \frac{V_t V_s}{X_L}\sin\delta \qquad (12)$$
$$Q = \frac{V_t}{X_L}(V_s\cos\delta - V_t) \qquad (13)$$

The turbine speed control is achieved via the control of active power of the generator. The output error of the speed controller set the command active power. Then, active power of the system is compared with the command active power. The output of the active power controller determines δ. Also, the output of the reactive power set m to produce the reference signal for PWM.

Commend reactive power and command speed are varied to investigate the system performance. Both reactive power and speed must track their commands. A step function and a constant value as the command of the reactive power are applied to the system. As it is shown in Fig.14 and Fig.15 reactive power tracks its references with no steady state error and in Fig.15 rise time is less than 100ms. The output of the reactive power controller, that is depicted in Fig.16, stay at the allowed range. Also, in order to test the system performance, a ramped shape command speed, corresponding to Fig.17, is applied to the system which angular speed tracks this command speed with a soft ramp. Maximum error in speed tracking is less than %1.

Results show the proposed wind turbine-generator and its control system, operate with acceptable accuracy. This proposed scheme can be a good candidate for wind systems.
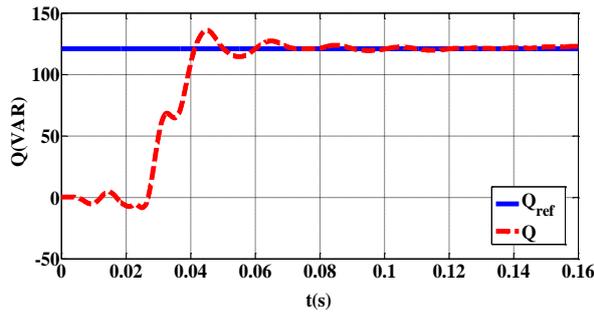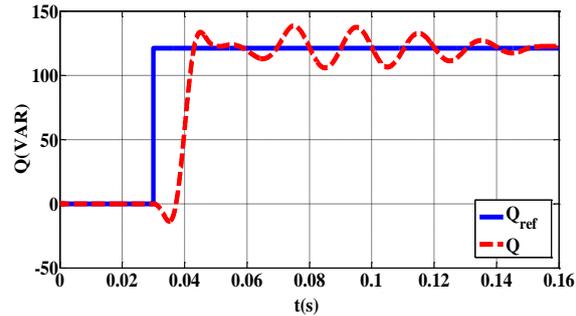
Fig.14. *reactive power and its constant reference*

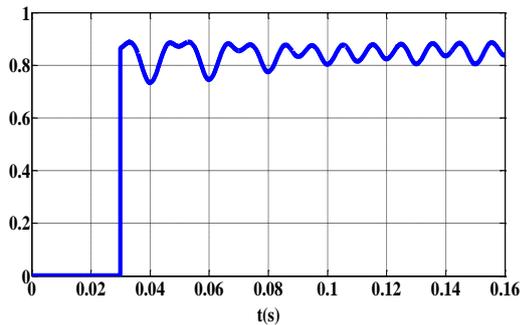**Fig.15.** *reactive power and its step command*

Fig.16. *output of the reactive power controller*
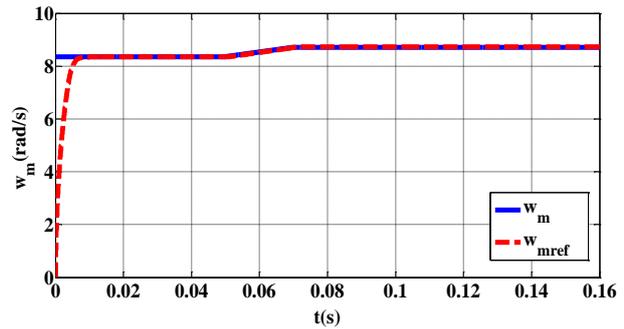

Fig.17. *angular speed and its reference*

Discussion: From equations (12) and (13), the active and reactive powers are varied by the variations of both δ and Vt. Since δ usually is a small angle and cos δ≈1, the variation of Q is more affected by the Vt. Also, by assuming that δ has a small amount, P can be controlled via δ.

4. CONCLUSION

An AFPM generator with distributed winding and circular magnet shape was modeled by 3D FEM as the generator of a direct drive wind system. Obtained results were used to simulate the considered low speed wind turbine. The system was connected to the network via a modular multilevel inverter. Two control methods, averaging control and balance control, were applied to protect the voltage balance of the capacitors. The commands of the reactive power and angular speed were changed to evaluate the performance of the system. reactive power as well as speed tracked their commands with a good accuracy. Results show the proposed system can be an acceptable design for low speed wind turbine-generators.

REFERENCES

[1] Camara, M. S., Camara, M. B., Dakyo, B., Gualous, H., " An offshore wind energy conversion system based on a Permanent Magnet Synchronous Generator connected to grid -modeling and control strategies", IEEE, Ecological Vehicles and Renewable Energies (EVER), pp. 1-6, 2015.

[2] Zhao, F., Lipo, T., A., Kwon, B., " A novel dual-stator axial-flux spoke-type permanent magnet vernier machine for direct-drive applications", IEEE Transactions on Magnetics, Vol. 50, Issue 11, 2014.

[3] Patil, K., Mehta, B., " Modeling and Simulation of Variable Speed Wind Turbine with Direct Drive Permanent Magnet Synchronous Generator", IEEE, ICGCCEE, pp. 1-6, 2014.

[4] Yang, L., Yan, S., Chen, Z., Liu, W., " A Novel Wind Turbine Simulator for Wind Energy Conversion Systems Using an Permanent magnet synchronous motor", IEEE, Inter. Conf. on Elec. Machines and Systems, Oct. 26-29, 2013, Busan, Korea.

[5] Li, L., Wang, T., Wang, X., "Dynamic Equivalent Modeling of Wind Farm with DDPMSG Wind Turbine Generators", IEEE, POWERCON, pp. 2908-2914, 2014.

[6] Jia, S., Qu, R., Li, J., Fan, X., " Study of Direct-Drive Permanent-Magnet Synchronous Generators With Solid Rotor Back Iron and Different Windings", IEEE Transactions on Industry Applications, Vol. 52, No.2, pp. 1369-1379, 2015.

[7] Wen, G., Chen, Y., Zhong, Z., Kang, Y., " Dynamical voltage and current assignment strategies of nine-switch-converter-based DFIG wind power system for low voltage ride through (LVRT) under symmetrical grid voltage Dip", IEEE Transactions on Industry Applications, Vol. PP, Issue 99, 2016.

[8] Daghigh, A., Javadi, H., Torkman, H., " Design Optimization of Direct-Coupled Ironless Axial Flux Permanent Magnet Synchronous Wind Generator with Low Cost and High Annual Energy Yield", IEEE Transactions on Magnetics, Vol. PP, Issue 99, 2016.

[9] Virtic, P., Vrazic, M., Papa, G., " Design of an Axial Flux Permanent Magnet Synchronous Machine Using Analytical Method and Evolutionary Optimization", IEEE Transactions on Energy Conversion, Vol.31, Issue 1, pp. 150-158, 2015.

[10] Khan, M. S. U., Maswood, A. I., Tafti, H. D., Roomi, M. M., " Control of bidirectional DC/DC converter for back to back NPC-based wind turbine system under grid faults", IEEE, ICDRET, pp. 1-6, 2016.

[11] Ozdemir, S., Selamogullari, U., S., Elma, O., "Analyzing the effect of inverter efficiency improvement in wind turbine systems", IEEE, 3rd Inter. Conf. on Renewable Energy Research and Appl., 2014.

[12] Yaramasu, V., Wu, B., "Predictive control of a three-level boost converter and an NPC inverter for high-power PMSG-based medium voltage wind energy conversion systems", IEEE, Trans. On Power Elec., Vol. 29, No. 10, 2014.

[13] Iov, F., Blaabjerg, F., "Power Electronics and Control for Wind Power Systems", IEEE, PEMWA, pp. 1-16, 2009.

[14] Vinod, S., Navin, V., Sivaraj, C., "Simulation of power electronics based controller for grid connected wind turbine", IEEE, ICETECT, pp. 255-260, 2011.

[15] Thitichaiworakorn, N., Hagiwara, M., Akagi, H., " A medium-voltage large wind turbine generation system using an AC/AC modular multilevel cascade converter", IEEE Journal of Emerging and Selected Topics in Power Electronics, Vol. 4 , Issue 2, pp. 534-546, 2015.

[16] Vidal-Albalate, R., Beltran, H., Rolan, A., Belenguer, E., "Analysis of the Performance of MMC Under Fault Conditions in HVDC-Based Offshore Wind Farms", IEEE Transactions on Power Delivery, Vol. 31, Issue 2, pp. 839-847 , 2016.